Pergamon

Int. J. Multiphase Flow Vol. 24, No. 1, pp. 93–103, 1998

Printed in Great Britain
PII: S0301-9322(97)00041-4
0301-9322/98 $19.00 + 0.00

VOLUME FRACTION AUTOCORRELATION FUNCTIONS IN A TWO-PHASE BUBBLE COLUMN

E. SALINAS-RODRÍGUEZ[1], R. F. RODRÍGUEZ[2], A. SORIA[1] and N. AQUINO[3]

[1]Universidad Autónoma Metropolitana, Departamento I.P.H., Apartado Postal 55-534, 09340 Mexico D.F., Mexico

[2]Instituto de Física, Departamento de Física Química, UNAM, Apartado Postal 20-634, 01000 Mexico D.F., Mexico

[3]Universidad Autónoma Metropolitana, Departamento de Física, Apartado Postal 55-534, 09340 Mexico, D.F., Mexico

(Received 14 May 1996; in revised form 22 May 1997)

Abstract—We use an electrical impedance technique to measure the fluctuations of gas volume fraction in a gas–liquid bubble column in turbulent flow regime. From these experimental values the volume fraction autocorrelation function is determined. On the theoretical side, we introduce a stochastic model to describe the aggregation of bubbles by assuming them to be rigid spheres of different diameters and by considering their coalescence as a stochastic Markovian process. The coalescence rate contains one adjustable parameter which takes into account the neglected effects of compressibility and deformation, spatial inhomogeneities and hydrodynamic interactions between the bubbles and with the boundaries. The associated master equation for this polydispersed system is built up, and from it we derive an equation for the volume fraction equilibrium correlation functions for several bubble sizes. By adjusting the free parameter, we compare the theoretical correlations with corresponding experimental values and find that the standard deviation associated with their difference can be made as small as 0.017. We discuss the limitations and possible generalizations of our model and conclude by making further physical remarks.

Key Words: bubble column, correlation function, multiphase flow, aggregation phenomena

1. INTRODUCTION

Bubble columns are industrial equipment filled up with a liquid and a gas. The liquid phase flows as a continuous phase while the gas flows as a set of dispersed bubbles. Many chemical heterogeneous reactors are bubble columns where reactions usually take place in the liquid phase, once a reactive chemical has been absorbed from a gaseous stream through the interfacial films between bubbles and liquid. Bubble columns can also contain solid particles in the liquid stream. Depending upon the solid particle size and the device used to lift the particles, the reactor can be a slurry or a three-phase fluidized bed. Both petrochemical and environmental applications are important examples of the use of these reactors. Transient phenomena are important at the start-up of these equipments, and their analysis is important in order to characterize the dynamic behavior of the system and to get a better insight into the phenomena driving some events such as pattern transitions.

Bubble channels are also present in the nuclear reactor technology, known as BWR (boiling water reactor). Transient phenomena are of enormous importance in the operation of these reactors in order to prevent instabilities that could drive the system out of control and produce severe accidents. The dynamic characterization of the two-phase flow is therefore an excellent tool for the prevention of instabilities.

Transient analysis is built on the basis of data taken in records or time series, which are the most important experimental information required. Time series analysis has been mainly related with the identification of flow patterns. Electrical impedance signals are based on the discrimination of the electrical conductivity of the liquid and the gas. A primary voltage signal is thus obtained at a selected sampling frequency. For the purpose of later comparison of these experimental data with

theoretical predictions, we first express the time series in terms of a variable known as the void fraction. Then we compute the volume fraction autocorrelation functions. These quantities give the residence time t_r of a given signal in the measurement zone.

Although the calculation of correlation functions for gas–liquid systems is rather scarce in the literature, there exist some papers dealing with models of autocorrelation functions for gas–liquid systems in a horizontal column (Drahos *et al.* 1987) or for liquid–solid fluidized beds (Cermák *et al.* 1979; Yutani *et al.* 1983, 1986, 1987). The basic purpose of our work is to present a stochastic model which takes into account the possibility of coalescence between bubbles and that allows us to calculate volume fraction correlation functions. More specifically, since any event that leads to the spontaneous creation or annihilation of particles is strictly speaking a probabilistic event, it should be formulated in terms of probability distributions. However, a statistical description does not necessarily imply a stochastic approach. The essential difference lies in the importance of fluctuations in the chosen state variables. For instance, a stochastic description of a system with a small population is justified if the fluctuations in the number of particles are large. In this case it is necessary to know higher order moments of the probability distribution beyond its average. On the other hand, a system with a large population can be described statistically in terms of its average (deterministic) behavior only, if the fluctuations around the average number are and remain small so that they can be neglected. For systems in thermodynamic equilibrium, fluctuations in the state variable are known to be small; however, for nonequilibrium states they can increase and become an essential part of its dynamical behavior (Haken 1975). This is the case of disperse nonlinear multistable systems in the vicinity of gelation points (Family and Landau 1984; Salinas-Rodríguez and Rodríguez 1995), since these points represent the stability limit of the stationary states and the corresponding thermodynamic forces that maintain them vanish as the system is closer to the transition points. Therefore, since the magnitude of the fluctuations is a measure of the validity of a macroscopic description, and since in the experiments to be described below fluctuations turned out to be important, it is of interest both theoretically and practically to study fluctuation dynamics around the average behavior.

To this end the paper is organized as follows. In section 2 we first define the relevant experimental parameters and the flow pattern of the gas phase for which experimental measurements were carried out. Then the experimental set-up is described and we discuss how the time series were captured. The way in which the experimental volume fraction autocorrelation functions are computed from the void fraction time series is also established. In section 3 we introduce a stochastic model to describe the experimental observations by assuming that the observed coalescence of bubbles is a Markovian process. We then derive a time evolution equation for the probability density of this process and calculate the theoretical volume fraction correlation functions. Finally, in section 4 we compare our theoretical predictions with experimental observations and find good agreement expressed by very small values of the standard deviation. We conclude by pointing out some advantages, limitations and possible generalizations of our approach.

2. EXPERIMENTAL

2.1. *Experimental definitions and concepts*

The topological structure of a bubbling flow can be characterized by its geometric parameters known as the volume fraction of bubbles, sometimes referred to as the *void fraction* (ϵ_G), and the *specific interfacial area* (a_s) (Soria and De Lasa 1992). Both variables are absent in flows with only one phase. Bubble columns operate in a wide range of liquid and gas flow rates. The *superficial liquid velocity* (v_{SL}) is the liquid flow rate divided by the cross-section area of the column. This parameter is sometimes referred to as the *volumetric liquid flux*. A similar definition is also used for the *superficial gas velocity* (v_{SG}), also called the *volumetric gas flux*. The sum of both superficial velocities is the velocity of the mixture center of volume, known as the *mixture velocity* (v_0) or *total volumetric flux* (Wallis 1969).

While superficial liquid velocities in bubble column reactors usually go from zero up to 0.100 m/s, superficial gas velocities frequently range from 0.010 to 0.200 m/s, although sometimes high gas throughputs up to 0.400 m/s are operated. The dispersed gas phase takes on some specific configurations, called flow patterns, mainly depending on the gas flow rate. At low enough

superficial gas velocities a *homogeneous bubbling* (HB) flow pattern is observed, where bubbles are uniformly distributed inside the column. At high superficial gas velocities strong interactions between bubbles are observed and are manifested as interface deformations, bubble collisions and strong agitation. Strong liquid circulation is also observed. It is conventional to call this regime the *churn-turbulent bubbling* flow pattern (CTB). Both regimes can exist when the superficial liquid velocity vanishes, since liquid circulation is produced by the fast displacement of big bubbles and clusters of bubbles.

The transition between HB and CTB flow patterns can be characterized from a plot of ϵ_G vs v_{SG}. The rate of change of ϵ_G with respect to v_{SG} has two distinct asymptotic slopes, the larger one being characteristic of the HB regime and the smaller one corresponding to the CTB regime. It is apparent that flow patterns were not originally associated with specific ranges of a Reynolds number (Zahradník and Fialová 1996) as is frequently the case in hydrodynamics. Flow pattern identification has also been done through the statistical characterization of pressure drop signals (Glasgow *et al.* 1984; Drahos and Cermak 1989; Drahos *et al.* 1991) or void fraction signals (Micaelli 1982; Bernier 1982; Turnaire 1987; Kytömaa and Brennen 1988, 1991; Soria and De Lasa 1992) recorded at 10^2 to 10^3 Hz. In order to get those signals, electronic instruments such as piezoelectric pressure transducers or electrical impedance electrodes have been used.

2.2. *Experimental set-up*

The bubble column utilized was a Plexiglas vertical column, 0.20 m in diameter and 2.6 m in axial length above the distributor. The column was adapted with a set of electrodes, with the first measuring electrode placed 0.914 m above the distributor. The electrodes were flush to the inside walls of the column, as can be appreciated in figure 1. Five pairs of measuring electrodes were alternated with six pairs of guard electrodes. All electrodes were rectangles of 0.157×0.075 m^2 and each electrode of a pair was placed at π radians from the other at the column cross-section. The distributor was a brass grid with 1240 holes, 8×10^{-4} m in diameter, separated with an equilateral pitch of 5.0×10^{-3} m. A concentric pipe mixer was adapted upstream of the distributor in order to produce a two-phase air–water mixture, which impacted the distributor from below in a thin chamber, from which the two-phase mixture flowed through the holes (Soria and De Lasa 1992). The range of superficial gas velocity up to 0.0470 m/s and the superficial water velocity was maintained at 0.0197 m/s. This design allowed us to get a uniform swarm of air bubbles in the water stream (Soria 1991), which conserved its identity at low gas flow rates with scarce coalescence events. When high gas flow rates were established, bubbles or jets emerging from the distributor were observed to coalesce immediately, giving rise to the characteristic CTB regime. The transitions between HB and CTB regimes can be appreciated from our data in figure 2, taken at a constant superficial liquid velocity $v_{SL} = 0.0197$ m/s. Two straight lines can be drawn for the data shown, crossing around the point $v_{SG} = 0.0100$ m/s and $\epsilon_G = 0.15$. This point is close to the transition between the mentioned flow patterns.

2.3. *Data treatment*

Time series were captured at a frequency of 100 Hz in a time of 10 s. This sampling frequency was selected, according to the Nyquist frequency, in order to capture most of the relevant phenomena relative to the motion of void fraction waves (Bernier 1982; Turnaire 1987; Saiz-Jabardo and Bouré 1989; Soria 1991; Soria and De Lasa 1992). Simultaneous time series were captured, one for each of the first two measuring levels. Then the primary time series were changed to the corresponding void fraction time series by using a Maxwell algorithm (Maxwell 1904) adapted with an adjustable constant which accounted for errors in the physical sizes of the electrodes. Experimental void fraction time series can be observed for a homogeneous bubbling regime (HB regime) and for a churn-turbulent regime (CTB regime) in figure 3.

Experimental autocorrelation functions $E^{exp}(t)$, that is those measured in the same section of the column, were computed for void fraction time series according to the definition.

$$E^{exp}(j) = \frac{1}{1000 - j} \sum_{i=0}^{1000-j} \epsilon_G(i)\epsilon_G(i+j) \qquad [1]$$

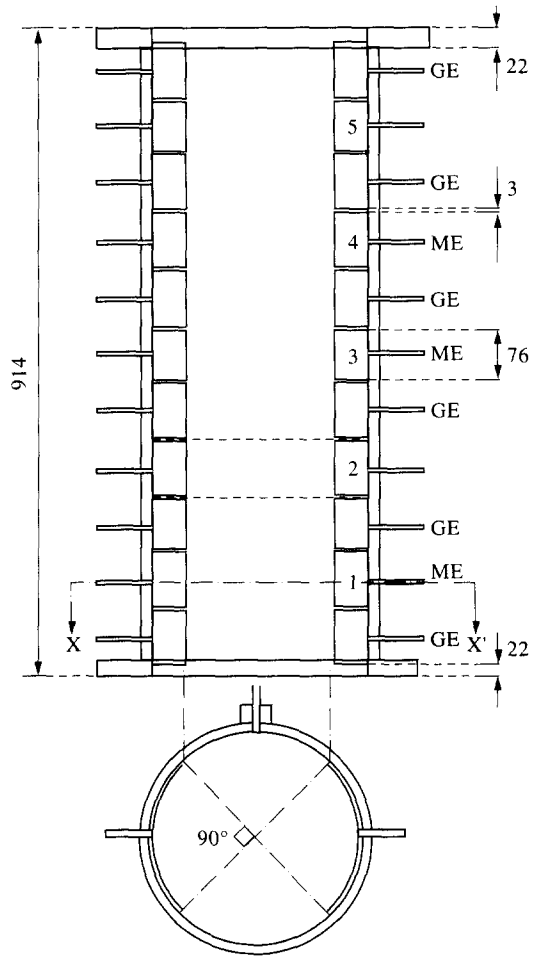

Figure 1. Schematic representation of the XX′ plane of the bubble column, where the diameter of the circle indicates the XX′ section (- . - .). The section between the dashed lines indicates the measuring zone for electrodes, level 2. All dimensions are in millimeters. GE and ME denote, respectively, the guard and measuring electrodes.

where j is a time lag index which divided by the sampling frequency gives the time lag in seconds. It should be stressed that these autocorrelations are estimated for each of the measuring levels and are normalized with respect to the value $E_0 \equiv E(j = 0)$.

Normalized autocorrelations are shown in figure 4 for CTB. They show that for short times the autocorrelation function values are large; in this case they mainly give information about the residence of a void fraction signal in the measuring influence zone. In contrast, for large times the autocorrelations are weaker and contain both the influence of uncontrollable noise effects and the dynamic characteristics of the electrical measuring technique, since the electric potential measuring volume changes slightly depending on the presence of bubbles in the measuring surroundings. In this work we will identify the residence time t_r with point A in figure 4, which defines the lowest autocorrelation value after removing the part of the signal contained between the dashed lines. Clearly, this definition is not unique, but later on we will use it consistently in the theoretical calculations.

3. THEORETICAL CONSIDERATIONS

3.1. *Model and basic equations*

A characteristic initial bubble diameter was estimated from the experimental void fraction propagation speed relative to the mixture velocity. The value of this parameter is in the order of

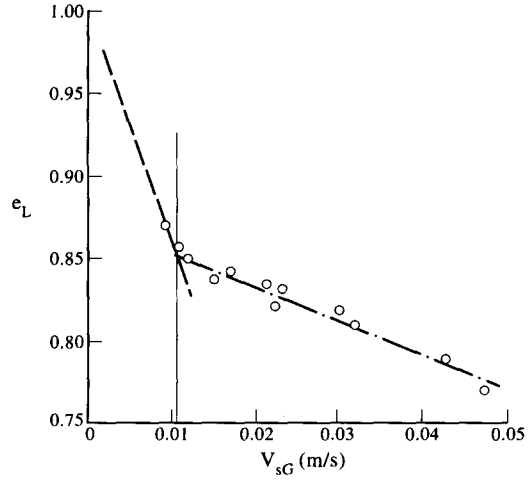

Figure 2. Liquid volume fraction ϵ_L vs v_{sg} for homogeneous bubbling (- - -) and churn-turbulent bubbling (- . - . -) flow patterns for $v_{SL} = 0.0197$ m/s. The circles denote experimental values.

0.15 m/s (Soria 1991; Soria and De Lasa 1992). Therefore taking this velocity as an approximation to the terminal velocity of the bubbles, whose expression using Stokes approximation for a sphere is $v_{TG} = 2R^2(\rho_L - \rho_G)g/(9\mu_L)$ (Bird *et al.* 1960; Gaddis and Vogelpohl 1986). Here μ_L is the dynamic viscosity of water, ρ_L and ρ_G are the water and air densities, respectively, and R is the bubble radius. For air–water flow at room temperature, the bubble radius turned out to be $R = 2.6 \times 10^{-3}$ m, approximately.

In the first and second measuring levels of the bubble column, where all the measurements were carried out, we assume that there are N spherical and rigid air bubbles at time t. A state of the bubbles is characterized by each realization of the size distribution $\{m_k\}$, where m_k denotes the number of bubbles of size k. According to the observations described in the previous section, the sizes of the bubbles increase, approximately, up to 2 or 3 times their initial size in the CTB regime; therefore, we assume that $k = 1$, 2 and 3 only. When the bubbles come randomly into contact among themselves they coalesce or adhere to one another, changing the size distribution $\mathbf{m} \equiv \{m_k\}$. Thus, the vector $\mathbf{m}$ is a stochastic variable with a probability distribution function $P(\mathbf{m}, t)$ which represents the probability that the number of bubbles of size k at time t is given by m_k when the system is considered to be spatially homogeneous.

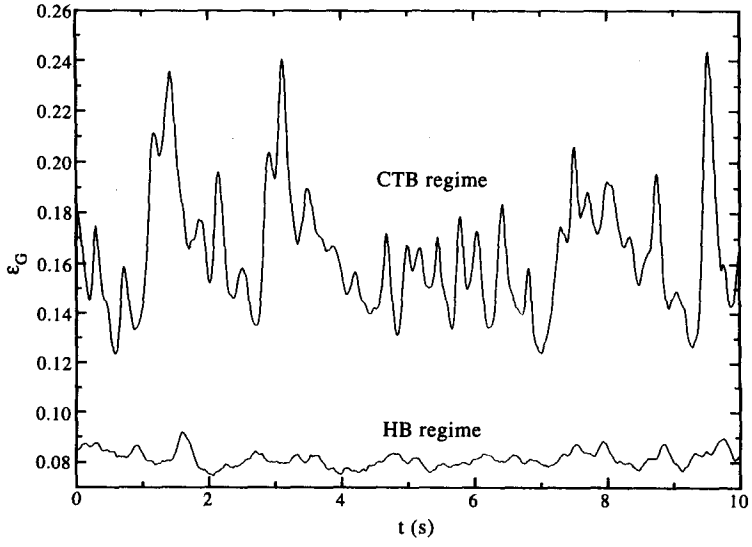

Figure 3. Time series for void fraction function ϵ_G for HB and CTB regimes.

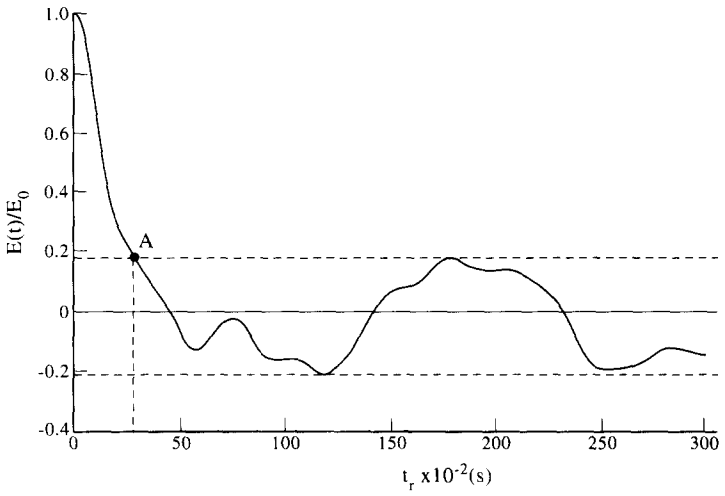

Figure 4. Normalized experimental volume fraction autocorrelation function for CTB regime. Point A indicates the experimental residence time.

The coalescence of bubbles will be modeled as a Markovian stochastic process described by the probability distribution function $P(\mathbf{m}, t)$. Then the time evolution of $P(\mathbf{m}, t)$ is governed by the following master equation (van Dongen and Ernst 1987; Salinas-Rodríguez 1992; van Kampen 1993):

$$\frac{\partial}{\partial t} P(\mathbf{m}, t) = \frac{1}{2V} \sum_{i,j=1}^{\infty} K_{ij} \Delta_{ij} [P(\mathbf{m}, t)(m_j - \delta_{ij}) m_i] \qquad [2]$$

where $V \equiv V_L + V_G$ is the volume of the liquid–gas mixture contained in the section of the column under consideration and the operator Δ_{ij} is defined by

$$\Delta_{ij} f(\mathbf{m}) \equiv f[\{m_k + (\delta_{ik} + \delta_{ij} - \delta_{i+j,k})\}] - f(\mathbf{m}) \qquad [3]$$

where $f(\mathbf{m})$ is an arbitrary function of $\mathbf{m}$ and δ_{ik} is the usual Kronecker delta.

The coalescence kernel K_{ij} denotes the probability per unit time that two bubbles of sizes i and j coalesce to produce a bubble of size $i + j$ (Salinas-Rodríguez *et al.* 1991; Blackman and Marshall 1994; Blackman 1995; Leyvraz 1995). Clearly, K_{ij} should be a function of the sizes i and j and its explicit form depends on the specific mechanism of coalescence. Thus, given K_{ij} the essential problem consists in solving [2] for a given initial distribution $P^0(\mathbf{m}) \equiv P(\mathbf{m}, t = 0)$.

Since the volume fraction $\epsilon = V_G/V$ and V can be measured, the initial number of bubbles $N_0 \equiv N(t = 0)$ can be estimated to be $N_0 = \epsilon V/V_1$, where V_1 is the volume of one spherical bubble of an initially monodisperse swarm of bubbles. Therefore N_0 turns out to be $N_0 \approx 5300$ for the CTB regime.

As the bubbles enter the section of the column where the measurements are carried out, they coalesce. For the observed CTB regime we shall assume that K_{ij} may be modeled by the turbulent coalescence kernel K_{ij}^T, whose expression was derived by Saffman and Turner (1956) in the modeling of the coalescence of droplets in clouds. They considered an isotropic fully developed turbulent flow and assumed that the size of the dispersed phase is smaller than the length scale of the smallest eddies. This leads to

$$K_{ij}^T = \beta (i + j)^3 \qquad [4]$$

where $\beta \equiv \beta' \xi / \nu$. Here ξ is the rate of energy dissipation per unit mass, ν is the kinematic viscosity of water, $\nu \equiv \mu_L/\rho_L$, and β' is also an adjustable parameter which accounts for corrections due to the neglected deformation and compressibility effects. Actually, later on we shall rather adjust the value of β instead of that for β' to compare our calculations with our experimental results.

3.2. *Volume fraction correlation function*

The moments of $P(\mathbf{m}, t)$ are defined by

$$\langle m_k^v(t)\rangle \equiv \sum_k m_k^v(t) P(\mathbf{m}, t). \tag{5}$$

Time evolution equations may be derived from [2] by multiplying each term by $m_k^v(t)$ and summing over all possible states k. For the first moment this yields

$$\frac{\partial}{\partial t}\langle m_k(t)\rangle = \frac{1}{2V}\sum_{i,j=1}^{\infty} K_{ij}\Delta_{ij}\langle m_i\rangle\langle m_j\rangle. \tag{6}$$

Now, if the size distribution function or distribution of the average sizes of clusters is defined as

$$C_k(t) \equiv \frac{\langle m_k(t)\rangle}{V} \tag{7}$$

[6] may be rewritten as

$$\frac{\mathrm{d}}{\mathrm{d}t} C_k(t) = \frac{1}{2V}\sum_{i,j=1}^{\infty} K_{ij}\Delta_{ij} C_i C_j \tag{8}$$

or using [3] as

$$\frac{\mathrm{d}}{\mathrm{d}t} C_k(t) = \frac{1}{2}\sum_{j=1}^{k-1} (K_{j,k-j} C_j C_{k-j}) - \sum_{j=1}^{\infty} K_{kj} C_k C_j. \tag{9}$$

This is the well-known Smoluchowski equation (Smoluchowski 1916; Friedlander 1977), which is the usual starting point in a statistical description of the aggregation processes occurring in a variety of systems. Incidentally, the derivation of [9] from [2] shows that this commonly used approach is a particular case of our stochastic description (van Dongen and Ernst 1987; Salinas-Rodríguez 1992).

The size autocorrelation function is defined as

$$\kappa_{sk}(t) \equiv \langle\langle m_s(t) m_k(t)\rangle\rangle \equiv \sum_{\mathbf{m}} m_k m_s P(\mathbf{m}, t). \tag{10}$$

This quantity is a measure of the influence (correlation) that a bubble of radius s produces on one of radius k. If each term of [2] is multiplied by $m_k m_s$ and summed over all the possible values of m, one arrives at the following equation for κ_{sk}:

$$\frac{\mathrm{d}}{\mathrm{d}t}\kappa_{sk}(t) \equiv \sum_{j=1}^{\infty} A_{sj}\kappa_{jk}(t) + A_{kj}\kappa_{js}(t) \tag{11}$$

with

$$A_{kj}(t) \equiv \frac{1}{V}\sum_{i=1}^{\infty} K_{ij}(\delta_{ik} + \delta_{jk} - \delta_{i+j,k}) C_j(t) \tag{12}$$

and where C_j is the size distribution function defined by [8].

Now, in order to relate κ_{sk} with the volume fraction autocorrelation function $E(t)$ introduced in section 2.3, we first define the fluctuations of the volume fraction $\epsilon(t)$ with respect to a stationary mean value $\langle\epsilon\rangle$ as

$$\delta\epsilon(t) \equiv \epsilon(t) - \langle\epsilon\rangle. \tag{13}$$

In this way, the autocorrelation function of the fluctuations $\delta\epsilon(t)$ is given by

$$E(t) \equiv \langle\langle \delta\epsilon(t)\delta\epsilon(0)\rangle\rangle \equiv \langle \epsilon_0 \langle \delta\epsilon(t)\rangle_{\epsilon_0}\rangle \quad [14]$$

where $\epsilon_0 \equiv \epsilon(0)$ is the initial value of the volume fraction and the subscript ϵ_0 in angular brackets denotes a conditional average on the initial value ϵ_0.

On the other hand, since

$$V_G(t) = \sum_j V_j m_j(t) \quad [15]$$

where V_j and m_j are, respectively, the volume and number of bubbles of size j at time t, from [10] it follows that the volume fraction autocorrelation function is related with κ_{ij} by

$$E(t) = \frac{1}{V} \sum_{i,j} V_i V_j \kappa_{ij}(t) \equiv \sum_{i,j} E_{ij}(t). \quad [16]$$

It should be emphasized that while κ_{ij} is the size correlation, [10], $E_{ij}(t)$ is the volume fraction correlation function for bubbles of two different volumes. It measures how one bubble of volume i influences another bubble of volume j. This expression offers the possibility of comparing the measured values of $E^{exp}(t)$ given by [1] with the theoretical values $E^{theo}(t)$ obtained from [11] and [16]. More explicitly, for this purpose it is necessary to first solve [9] for a given initial size distribution function, $C_k(t = 0)$. As previously mentioned, an initial monodisperse size distribution was assumed for computations. This fact means that we are lumping the whole effective coalescence process, given from the distributor up to the measuring level, as if it were virtually given in the measuring zone. While this assumption enhances the importance assigned to coalescence, as computed by the model, the mechanisms considered by the particular choice of the coalescence kernel κ_{ij} remain valid. Thus, it is reasonable to assume that the initial size distribution is monodisperse:

$$C_k(t = 0) = N_0 \delta_{1k} \quad [17]$$

where N_0 is the initial number of bubbles. Then, substitution of the solution of Smoluchowski's equation [9] into [12] yields $A_{kj}(t)$. If the resulting expression for $A_{kj}(t)$ is then inserted into [11] and, consistently with [17] we also assume that

$$\kappa_{ij}(t = 0) = \frac{V}{v_1^2} E(t = 0)\delta_{ij} \quad [18]$$

[11] can be solved numerically and $E(t)$ is afterwards calculated from [16]. $E(t = 0)$ is obtained from the experimental data according to [1]. The numerical solution of [9] and [11] is obtained by using the D_{gear} routines from the IMSL routine package.

4. RESULTS AND DISCUSSION

Following the procedure outlined above, we calculated $E^{theo}(t)/E_0$ and plotted it against the residence time t_r, defined previously, as shown in figure 5 for the CTB regime. The corresponding values of $E^{exp}(t)/E_0$ are also shown in the same figure as measured in the second section of the column. It is important to emphasize once more that in our model there is only one free parameter, β, for the considered flow regime, whose value, owing to the physical interpretation given in the previous section, has to be adjusted to obtain good agreement between theory and experiment. To obtain these curves, the so-far unspecified parameter β introduced in [4] was determined by minimizing the standard deviation between the experimental time series and theoretical curve. This was achieved with the value $\beta = 1.5 \times 10^{-7}\ s^{-1}\ m^{-3}$. The standard deviation or average error is the difference between the experimental, $E^{exp}(i\delta t)$, and theoretical, $E^{theo}(i\delta t, \beta)$, values for the same time $i\delta t$, where β is our parameter to be adjusted. Then, a measure of our theoretical method with respect

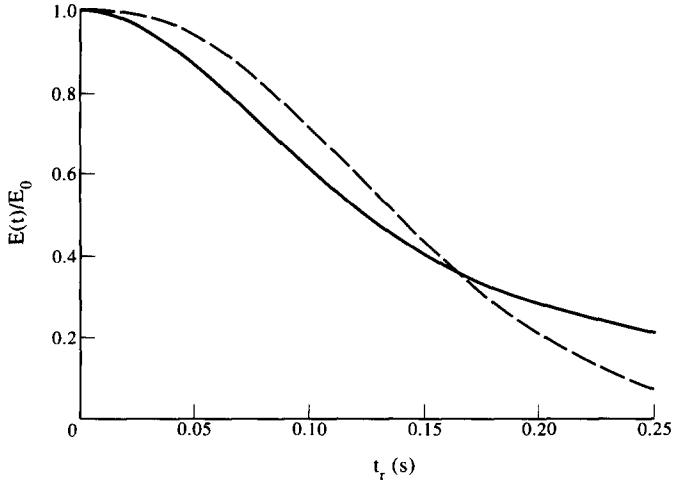

Figure 5. $E(t)/E_0$ vs residence time t_r for CTB regime; (—) experimental values, (- - -) theoretical curve.

to the experimental data is given by $[\Sigma_{i=1}^{N} (E^{\text{theo}}(i\delta t) - E^{\text{exp}}(i\delta t))^2]$. The standard deviation or average error of the estimation is defined as (Bevington and Robinson 1992)

$$\sigma = \left[\sum_{i=1}^{N} (E^{\text{theo}}(i\delta t) - E^{\text{exp}}(i\delta t))^2 / N \right]^{1/2} \qquad [19]$$

where δt is the time step selected for the integration of the system of differential equations, and $N\delta t$ is the total time of simulation. σ turned out to be $\sigma = 0.07$ for CTB. This expression, [19], estimates the statistical average error of our theoretical autocorrelation functions with the experimental data.

To see that the probability of coalescence between bubbles of different sizes is not the same, let us define the normalized volume fraction correlation function e_{ij} as $e_{ij}(t) \equiv E_{ij}(t)/E_0$. As mentioned earlier, this quantity measures the correlation between bubbles of different volumes. If we plot $e_{ij}(t)$ vs t_r for CTB, we obtain the curves in figure 6. They show that, consistently with the assumption of the monodisperse initial size distribution, at the beginning the strongest correlation is between bubbles of the same initial size, that is e_{11}. However, as t_r increases, correlations e_{12}, e_{13}, e_{22}, e_{23} and

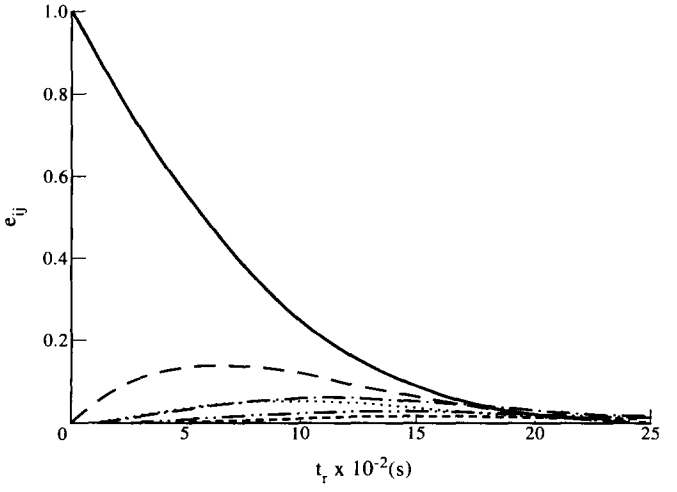

Figure 6. Normalized volume fraction correlation functions $e_{ij}(t)$ vs residence time t_r for CTB regime: (-) e_{11}; (- -) e_{12}; (· · ·) e_{13}; (- · -) e_{22}; (- · · -) e_{23}; (- - -) e_{33}.

e_{33} build up between bubbles of the new volumes that appear due to coalescence, but clearly they do not have the same weight in the total correlation $E(t) \equiv \Sigma_{i,j} e_{ij}$. We should stress at this point that the assumption of a monodisperse size distribution for each of the measuring levels could introduce severe limitations to the present discussion since the coalescence process takes place in the whole column.

At this point it is convenient to emphasize that the probabilities of coalescence K_{ij} should really be determined by taking into account many effects that have been neglected in our analysis. For instance, they may depend on the spatial position in the cell and they should also be affected by deformation effects. Furthermore, compressibility, spatial inhomogeneities and hydrodynamic interactions between bubbles and with the boundaries should be taken into account as well. However, given the complexity of these effects and of the system itself, this simple model seems to be a good first step in modeling the complex behavior of a bubble column in CTB flow regime.

On the one hand, we should stress again that the results obtained with this model show that the agreement between the experimental and theoretical values of $E(t)$ is good, with standard deviation as low as 0.017. This fact reinforces the point of view advocated above in the sense that the coalescence of bubbles may be considered as a stochastic Markovian process.

In this work we have only analyzed the coalescence of bubbles in the second section of the column for which an initial monodisperse size distribution has been proposed. While this assumption has proved to be reasonable, some improvement might be reached if different initial distributions are considered at the upper levels of the bubble column (Rodríguez *et al.* 1997).

It is also worth emphasizing once more that the definition of the residence time t_r is not unique. For instance, from the experimental curve in figure 4, t_r could be defined as well as the asymptotic intersection of the tangent line through point A with the time axis. Alternatively, it may also be defined as the first intersection of the autocorrelation function with the time axis. However, the point we want to stress is that our theoretical analysis has been carried out consistently with the definition of t_r given in section 2. Whether further generalizations of our model or different definitions of t_r than the one we have adopted are more useful remains to be assessed.

Acknowledgements—The authors would like to thank Professor Hugo Y. De Lasa from CREC, The University of Western Ontario, who kindly provided the facilities of his laboratory for the experiments reported here. Dr J. M. Zamora from U.A.M.I. is also acknowledged for providing a former computer code. This work has been partly supported by CONACyT, Mexico, through Grant 400200-5-3444A.

REFERENCES

Bernier, R. J. N. (1982) Unsteady two-phase flow instrumentation and measurement. Ph.D. Thesis, California Institute of Technology.

Bevington, P. R. and Robinson, D. K. (1992) *Data Reduction and Error Analysis for the Physical Sciences*, 2nd edn. McGraw-Hill, New York.

Bird, R. B., Stewart, W. E. and Lightfoot, E. N. (1960) *Transport Phenomena*. John Wiley, New York.

Blackmann, J. A. and Marshall, A. (1994) Coagulation and fragmentation in cluster–monomer reaction models. *J. Phys. A* **27,** 725–740.

Blackman, J. A. (1995) Growth models for discontinuous films. *Physica A* **220,** 85–98.

Cermák, J., Kastánek, F. and Havlícek, A. (1979) Statistical pressure characteristics in modelling of gas–liquid reactors. *Collect. Czech. Chem. Commun.* **42,** 56–68.

Drahos, J., Cermak, J., Selucky, K. and Ebner, L. (1987) Characterization of hydrodynamics regimes in horizontal two-phase flow. II. Analysis of wall pressure fluctuating. *Chem. Eng. Process* **22,** 45–52.

Drahos, J. and Cermak, J. (1989) Diagnostics of gas–liquid flow patterns in chemical engineering systems. *Chem. Eng. Process* **26,** 147–164.

Drahos, J., Zahradnik, J., Puncochár, M., Fialová, M. and Bradka, F. (1991) Effect of operating conditions on the characteristics of pressure fluctuations in a bubble column. *Chem. Eng. Process* **29,** 107–115.

Family, F. and Landau, D. P. (eds) (1984) *Kinetics of Aggregation and Gelation*. Elsevier, Amsterdam.

Friedlander, S. K. (1977) *Smoke, Dust and Haze*. John Wiley, New York.

Haken, H. (1975) Cooperative phenomena in systems far from thermal equilibrium and in nonphysical systems. *Rev. Mod. Phys.* **47,** 67–121.

Gaddis, E. S. and Vogelpohl, A. (1986) Bubble formation in quiescent liquids under constant flow conditions. *Chem. Eng. Sci.* **41,** 97–105.

Glasgow, L. A., Erickson, L. E., Lee, C. H. and Patel, S. A. (1984) Wall pressure fluctuations and bubble size distributions at several positions in an airlift fermentor. *Chem. Eng. Commun.* **29,** 311–336.

Kytömaa, H. K. and Brennen, C. E. (1988) Some observations of flow patterns and statistical properties of three component flows. *J. Fluid Engng.* **110,** 76–84.

Kytömaa, H. K. and Brennen, C. E. (1991) Small amplitude kinematic wave propagation in two-component media. *Int. J. Multiphase Flow* **17,** 13–26.

F. Leyvraz (1995) Scaling theory of aggregation. In *Dynamics of Nonlinear and Disordered Systems*. World Scientific, Singapore and references cited therein.

Maxwell, J. C. (1904) *A Treatise on Electricity and Magnetism I*, 3rd edn. Clarendon Press, Oxford.

Micaelli, J. C. (1982) Propagation d'ondes dans les écoulements disphasiques à bulles à deux constituants. Thesis, Université Scientifique et Mèdicale et Institut National Polytechnique de Grenoble, France.

Rodríguez, R. F., Soria, A., Salinas-Rodríguez, E. and Aquino, N. (1997) in preparation.

Saffman, P. G. and Turner, J. S. (1956) On the collision of drops in turbulent clouds. *J. Fluid Mech.* **1,** 16–30.

Saiz-Jabardo, J. M. and Bouré, J. A. (1989) Experiments on void fraction waves. *Int. J. Multiphase Flow* **15,** 483–493.

Salinas-Rodríguez, E., Rodríguez, R. F. and Zamora, J. M. (1991) Stochastic dynamics of spatial effects in fragmentation clusters. *Rev. Mex. Fis.* **37,** S51–S62.

Salinas-Rodríguez, E. (1992) Descripción estocástica de fenómenos de agregación. Ph.D. Dissertation, Universidad Autónoma Metropolitana, Mexico (in Spanish) and references cited therein.

Salinas-Rodríguez, E. and Rodríguez, R. F. (1995) Stochastic description of disperse systems. *Rev. Mex. Fis.* **41,** 431–450.

Smoluchowski, M. V. (1916) Drei Vortrage Uber Diffusion, Brownsche Bewegung und Koagulation von Kolloidteilichen. *Phys. Z.* **17,** 557–584.

Soria, A. (1991) Kinematic waves and governing equations in bubble columns and three-phase fluidized beds. Ph.D. Thesis, The University of Western Ontario, London, Ontario, Canada.

Soria, A. and De Lasa, H. (1992) Averaged topological equations for dispersed two-phase flows. *Int. J. Multiphase Flow* **18,** 943–964.

Turnaire, A. (1987) Détection et étude des ondes de taux de vide en écoulement diphasique à bulles jusqu'à la transition bulles-bouchon. Thesis, Université Scientifique et Médicale et Institut National Polytechnique de Grenoble, France.

van Dongen, P. G. J. and Ernst, M. H. (1987) Fluctuations in coagulating systems. *J. Stat. Phys.* **49,** 879–926.

van Kampen, N. (1993) *Stochastic Processes in Physics and Chemistry*. North Holland, Amsterdam.

Wallis, G. B. (1969) *One-dimensional Two-phase Flow*. McGraw-Hill, New York.

Yutani, N., Fan, L. T. and Too, J. R. (1983) Behavior of particles in a liquid–solids fluidized bed. *AIChE J.* **29,** 101–106.

Yutani, N., Ototake, N. and Fan, L. T. (1986) Stochastic analysis of fluctuations in the local void fraction of a gas–solids fluidized bed. *Powder Technol* **48,** 31–38.

Yutani, N., Ototake, N. and Fan, L. T. (1987) Statistical analysis of mass transfer in the liquid–solids fluidized beds. *Int. Eng. Chem. Res.* **26,** 343–347.

Zahradník, J. and Fialová, M. (1996) The effect of bubbling regime on gas and liquid phase mixing in bubble column reactors. *Chem. Eng. Sci.* **51,** 2491–2499.